Search for the decay of $\pi^0 \to \nu\overline{\nu}$
1/3 sample study
— Summary note —

K. Mizouchi

January 7, 2005

Contents

1 $\pi^0 \to \nu\overline{\nu}$ Signal Detection Strategy and Conceptional Design **6**

1.1 An upper limit equation and measured variables 6

2 E949 Detector and Triggers **7**

2.1 Data Sets 7

3 Analysis **9**

3.1 $K_{\pi 2}$ event purification and setup cut designing 9

3.1.1 Beam backgrounds suppression 9

3.1.2 Muon background suppression 13

3.1.3 The number of expected backgrounds in 1/3 sample 14

3.2 Online photon veto rejection 14

3.3 Online photon veto acceptance 17

3.3.1 $K_{\mu 2}$ sample selection criteria 17

3.4 Offline photon veto rejection and acceptance 19

3.4.1 Parameter scan and search for the most efficient cut set 20

3.5 Total photon veto rejection vs acceptance 21

3.6 The final photon veto cuts 22

3.7 Measurement of the track reconstruction disruption factor C_{dis} and hidden photon veto rejection in setup 23

3.8 Systematic errors in the measurements 25

3.9 Result — 1/3 sample 26

4 Single Photon Inefficiency Study **27**

4.1 Motivation and goal 27

4.2 A basic idea and an analysis strategy 27

4.3 Trigger and data set 28

4.4 Event purification and setup cut design 28

4.5 Photon reconstruction — clustering algorithm 29

4.5.1 Photon reconstruction performance 30

4.6 Tagging photon selection criteria 31

4.7 $K_{\pi 2}$ event reconstruction and missing photon kinematics 31
4.7.1 Kinematical fit with Lagrange multiplier 32
4.7.2 Event reconstruction with MC data set 32
4.8 Denominator Map 34
4.9 Numerator map 34
4.10 Normalization factor 34
4.11 Correction factors 35
4.12 Systematic errors in the table 36
4.12.1 Cell cross-talk matrix 36
4.12.2 Fake reconstruction 36
4.13 Single photon detection inefficiency — Result — 37

5 π^0 Detector Inefficiency in $K_{\pi 2}$ Decay 38
5.1 Daughter map generation 38
5.2 MC phase space generation and trigger bias correction 38
5.3 Result 39
5.3.1 Rejection as a function of π^+ dip angle 39
5.4 Discussion about the background mechanism 39

6 Background Expectation — 1/3 sample study 40
6.1 Expected number of backgrounds 40
6.2 Background distribution as a function of π^+ dip angle 40
6.3 Poisson based normal background subtraction 40
6.4 Background subtraction with unbinned extended maximum likelihood 40
6.5 Chi square fitting 40
6.5.1 David's technique 40

7 Preparation for 2/3 smaple study 41
7.1 Number of backgrounds prediction for 2/3 samples 41

List of Figures

1 BV early accidental hits 45
2 Online BV,BVL trigger occupancy and inefficiency 45
3 $K_{\pi 2}$-π^+ resolution. Total momentum, range, energy 46
4 Tagging photon resolution (MC clustering raw). E_{tag}, θ, ϕ 46
5 Tagging photon resolution (MC Lagrange multiplier fit). E_{tag}, θ, ϕ 47
6 missing photon resolution (MC Lagrange multiplier fit). E_{tag}, θ, ϕ 47
7 Chi square probability (MC recon) 47
8 Total π^0 rejection vs acceptance profile curve 48

List of Tables

1 $K_{\pi 2}$ event purification cuts 10
2 Single beam background bifurcation study (Rejection branch) 11
3 Single beam background bifurcation study (Normalization branch) 12
4 Two beam background bifurcation study (Rejection branch) 13
5 Two beam background bifurcation study (Normalization branch) 14
6 $K_{\mu 2}$, μ background bifurcation study 15
7 # of backgrounds in 1/3 sample 16
8 Online Photon Veto Rejection (HEX and HEX-afterburner) 16
9 Online Photon Veto Rejection (BV,BVL and EC) 17
10 Online Photon Veto Rejection (by trigger ratio method) 17
11 Online Photon Veto Rejection (BV,BVL and EC) with PSCUT02 18
12 Online Photon Veto Rejection (by trigger ratio method) with PSCUT02 18
13 $K_{\mu 2}$ event purification cuts 19
14 Online Photon Veto Acceptance (Layer18 method) 20
15 Online Photon Veto Acceptance (Blankout method) 20
16 Offline Photon Veto Cuts 22
17 Reconstruction disruption factor 23
19 Additional acceptance drop by HEX afterburner simulation with recorded trigger bits 25

18 table 25
20 Additional acceptance drop by recorded $\overline{\text{l0\_zfrf}}$ 26
21 Available run range for single photon inefficiency study 29
22 Available run range for single photon inefficiency study 30
23 Cluster reconstruction resolution (MC) 31
24 Input variables for Kinematical fit (MC) 33
25 Input variables for Kinematical fit (Real data) 34
26 1gamma trigger simulation to $K_{\pi 2}(1)$ data set 35
27 RSHEX+ rejection is L1.2 36
28 Single beam background bifurcation study (Rejection branch) : 2/3 sample . . . 41
29 Single beam background bifurcation study (Normalization branch) : 2/3 sample 42
30 Two beam background bifurcation study (Rejection branch) : 2/3 sample 42
31 Two beam background bifurcation study (Normalization branch) : 2/3 sample . 43
32 $K_{\mu 2}$, μ background bifurcation study : 2/3 sample 44
33 # of backgrounds in 2/3 sample 44

1 $\pi^0 \to \nu\overline{\nu}$ Signal Detection Strategy and Conceptional Design

$\pi^0 \to \nu\overline{\nu}$ signal detection starts with an identification of a π^0 surely existing in a detector volume. However, the direct detection is quite difficult since π^0 is a neutral particle and the life is extremely short, so that, it is necessary to catch the decay products or the generation process for the detection. The former method is taken in a beam dump experiment and has an advantage to certify π^0 certainly decays into neutrinos by detecting the neutrino interactions, but obviously it requires a large volume of detection device. E949 takes the latter way for the measurement. A well known Kaon decay process; $K^+ \to \pi^+\pi^0$ called $K_{\pi 2}$ is used for the π^0 identification by tagging K^+ and π^+. However, as you know, many K^+ decay modes involve a π^+ in their final products, the channel identification is done by two body decay kinematics with selecting stopped Kaons in an active target only. In regards to the π^0 decay, the neutrino detection is not available in the E949 experiment, however, with a hermetic veto, no final product interacts in the detection materials is confirmed for the signal identification. A point in here is, there is no check about the final products are neutrinos, any unknown particles which interacts only via weak force is acceptable. To summarize, $K_{\pi 2}$ decay but no π^0 activities are searched in this analysis.

Document overview Before moving into the next analysis section, a brief overview how the analysis proceeds in this document is mentioned here. Firstly, $K_{\pi 2}$ event purification is worked out in the section-3.1 and all required setup up cuts are designed there. Next, hermetic veto cuts are prepared in the section-3.6 and the inefficiency is measured with real data sample. After misc correction factors and systematics are studied in the section-3.7, upper limit with a conservative calculation is presented with 1/3 sample. To understand backgrounds coming through a detector photon inefficiency, detector inefficiency table is created with a special trigger data set in the section-4, and the tables are reworked to π^0 inefficiency in the section-5. Background subtraction with the measured π^0 inefficiency is performed in the section-6 and the improvement power is discussed with various statistical techniques Finally, a background estimation for remaining 2/3 sample is presented in the section-7.1.

One more thing to be noted here is; all figures are collected in the tail of this note.

1.1 An upper limit equation and measured variables

At first, conservative way of getting upper limit is shown here to make clear that what kinds of measurements are required for the analysis and make it a guideline for the following study.

Intrinsic $K_{\pi 2}$ acceptance with $K_{\pi 2}$ selection setup cuts is written as follows,

$$A_0 = \frac{N(K^+ \to \pi^+\pi^0)}{K_{sample1} Br(K^+ \to \pi^+\pi^0)} \tag{1}$$

where $K_{sample1}$ is a K_{BLive} and $Br(K^+ \to \pi^+\pi^0)$, $N(K^+ \to \pi^+\pi^0)$ are a branching ratio of $K_{\pi 2}$ and the number of remaining events after $K_{\pi 2}$ selection cut respectively. Considering further acceptance loss by photon related things, the acceptance is re-written as

$$A = A_0 C_{dis} C_{acc} \tag{2}$$

where C_{dis} is a disruption factor, which shows how often the π^+ reconstruction is disrupted by an existence of overlapping photons on the π^+ track and C_{acc} is a correction factor to recover signals which might be vetoed by photon veto cuts due to "*on-time*" accidental activities. Now, upper limit of the branching ratio is obtained by the following equation,

$$Br(\pi^0 \to \nu\bar{\nu}) < \frac{N_{90}}{K_{sample2} Br(K^+ \to \pi^+\pi^0) A} \tag{3}$$

where $K_{sample2}$ is the number of Kaons collected while our detector was alive and N_{90} is the number which Poisson statistics gives 90% confidence level in the case N events observed in the final box. Substituting the equation-1 and 2, the above equation becomes

$$\begin{aligned} Br(\pi^0 \to \nu\bar{\nu}) &< \frac{N_{90}}{N(K^+ \to \pi^+\pi^0)} \frac{K_{sample1}}{K_{sample2}} \frac{1}{C_{dis} C_{acc}} \\ &< \frac{N_{90}}{N(K^+ \to \pi^+\pi^0)} \frac{1}{C_{dis} C_{acc}} \end{aligned} \tag{4}$$

where, technically, the exact same Kaon data set is used to cancel out $K_{sample1}$, $K_{sample2}$. The first term "$N_{90}/N(K^+ \to \pi^+\pi^0)$" is a kind of π^0 inefficiency, namely equal to *1 / rejection*. The equation-4 tells us the upper limit can be fully obtained by measuring photon veto rejection and the acceptance (C_{acc}) with a correction factor of C_{dis}.

2 E949 Detector and Triggers

(E949 detector figure is snipped for the data size.)

2.1 Data Sets

For your reference, online triggers for the samples used in this analysis are listed below. Occasionally back to here and remind, if required.

$$\begin{aligned} K_{\pi 2}(1) &\equiv K_B \cdot T2 \cdot (6_{ct} + 7_{ct}) \cdot \overline{19_{ct}} && (5) \\ K_{\pi 2}(2) &\equiv K_{\pi 2}(1) \cdot IC \cdot DC \cdot HEX \cdot L1.n && (6) \\ PNN1 &\equiv K_{\pi 2}(2) \cdot \overline{BV + BVL + EC} \cdot (L0rr1(1) \cdot US + L0rr1(2) \cdot DS) \cdot \overline{\text{L0\_zfrf}} && (7) \end{aligned}$$

Because the final products are same as PNN1, for the signal exploration, PNN1 trigger was used. Analysis run range is limited only in (48077:50218) to pick out the mean-timer runs. $K_{\pi 2}(1)$ trigger and $K_{\pi 2}(2)$ trigger are used to measure the number of $K_{\pi 2}$ decays occurred in the detector.

3 Analysis

3.1 $K_{\pi 2}$ event purification and setup cut designing

Since the current upper limit of the Br($\pi^0 \to \nu\overline{\nu}$) is 8.3×10^{-7} and we aim to obtain one order better improvement, background control below 10^{-7} level is quite important for the measurement. If we want to lead our analysis to photon background subtraction with an intention of further improvement than what we can expect from our detector inefficiency, at least, we need to purify the sample as clean as the remaining backgrounds become only $\pi^0 \to \gamma\gamma$ decays surviving through the detector photon inefficiency.

There are two mandatory requirements for setup cuts when their designs are made; (1) Setup cuts must be independent of photon veto as much as possible because the measured rejection gets under-estimated if the setup cuts take over a part of the rejection. (2) As already mentioned, 10^{-7} level of purification is required especially for photon disassociate events since they are not vetoed by photon veto and have more possibility to survive in the final box. Before measuring a photon veto rejection, such kind of setup cuts must be designed beforehand.

Basically, PNN1 cuts are available except for PV part. Since the final products are exactly same as the products in this decay mode, and their design already achieved to $10^{-10} \sim 10^{-11}$ background level for $K^+ \to \pi^+\nu\overline{\nu}$ detection, it is quite enough for this study. However, some cuts have a correlation to PV, or rather directly use the PV related hits (for example, in the beam background cuts), such cuts must be carefully removed.

The designed setup cuts are summarize in the table-1. Because some cuts are removed and the phase space cuts are different from PNN1, the background estimation in the KP2BOX is performed here.

3.1.1 Beam backgrounds suppression

E949 ran under the beam condition of 4/1 K^+ to π^+ ratio with two mass separators, (it was down to 3/1 later due to the separator problems), the number of π^+ entering events are expected to be comparable with that of Kaon entering events in an order estimation. π^+ scattered into our detector volume must be well identified with a Cerenkov counter, a B4 dE/dX counter and delayed coincidence for the confirmation of Kaon decay because single pion scatter-in events can survive photon veto and pion decay sequence cuts, which means all cuts are passed other than beam related one.

The number of single beam backgrounds in the signal box Bifurcation analysis is taken for a measurement of the number of single beam backgrounds. Here, "single beam background" means the case π^+ beam particle scatters into the detector acceptance or the case one of the final product from a decay-in-flight K^+ scatters into. The basic idea of this type background estimation is that at first DELC rejection R_{DELC} to the single beam backgrounds is measured

Category	Cut Entry
RUN	BAD_RUN, $run \geqq 48077$
	discard runs : $48540 \leqq run \leqq 48575$
PASS1 cuts	DUPEV, TRBIT, LEV11, LEV12, RD_TRK, STLAY, BAD_STC, RSHEX, TRKTIM, UTC, RDUTM, PDC, LAY14, UTC1, RANGE1, RSHEX2, TARGET
skim1, 4 selection	FITPI, PSCUT, TGCUT, (PRESCALE3)
$K_{\pi 2}$ box cuts	$\lvert ptot - P_{peak}\rvert < 3 \times \sigma_{ptot}$, $P_{peak} = 205.0$, $\sigma_{ptot} = 2.295$
	$\lvert rtot - R_{peak}\rvert < 3 \times \sigma_{rtot}$, $R_{peak} = 30.33$, $\sigma_{rtot} = 0.8738$
	$\lvert etot - E_{peak}\rvert < 3 \times \sigma_{etot}$, $E_{peak} = 109.0$, $\sigma_{etot} = 3.158$
Kinematic cuts	
	ICODEL14, UTCQUAL, RNGMOM, PIGAP
— Fiducial —	COS3D, LAYV4, ZFRF, ZUTOUT
— RS dE/dX —	RSDEDXCL, RSDEDXMAX, RSLIKE
— PRRF —	PR_RF, PR_RF_XY, PR_RFZ1, PR_RFZ2
— TGLIKE —	TGLIKE1, TGLIKE2
— TGDB4 —	TGDB4, TGDB4TIP, TGDVXTIP, TGDVXPI
π^+ decay chain cuts	
	IPIFLG, EV5, TDFOOL, TDVARNN
Beam background cuts	
	DELC, KIC
— TG pattern —	TGQUALT, TGZFOOL, TARGF, DTGTTP, RTDIF, DRP
— B4BWBH —	B4DEDX, BWTRS, B4ETCON, B4TRS, B4CCD
— Cerenkov —	CPITRS, CPITAIL, CKTRS, CKTAIL
— TG energy —	B4EKZ
— Timing —	TIMCON, TGTCON, TIC

Table 1: $K_{\pi 2}$ event purification cuts

by tagging/enhancing the backgrounds with B4 dE/dX (B4AMB) cut in the rejection branch, and then, after inverting the DELC cut, the number of events remaining in the final box ($N_{\pi^+ \text{beam}}$) is measured. The expected backgrounds is given by $N_{\pi^+ \text{beam}}/(R_{DELC} - 1)$.

The table-2 shows the flow of the rejection branch. Basically in a bifurcation analysis, all cuts other than what one wants to measure must be imposed as setup to leave/isolate the beam backgrounds only, however, TGPV in photon veto cuts is turned off since the target photon veto affects the beam background study (, rejection tends to be underestimated because TGPV vetoes the target activities). TD cuts and some of kinematics cuts are also skipped because DELC rejection is large and it is distressed by a lack of statistics if all are imposed. As shown in the table-2, to enhance single beam backgrounds in the sample, smaller dE/dX events compare to typical Kaon energy deposit are selected by imposing B4ABM<1.0 MeV. Also PNN1BOX

Description	PNN1 PASS1 prescale 3		
Kin, TD, PV setup cuts Beam related setup cuts	UTCQUAL, RNGMOM, COS3D, LAYV14, ZFRF, ZUTOUT, PV (no TGPV) TGQUALT, TGZFOOL, TARGF, DTGTTP, RTDIF, DRP, KIC, BWTRS, B4ETCON, B4TRS, B4CCD, TIMCON, TGTCON, TIC entry : 1300289		
π^+, μ beam tag	B4ABM $<$ 1.0, PNN1BOX entry : 19241		
Misc. cuts	All Kin * All TD entry : 4172	All TD entry : 12258	— NO — entry : 19241
	DELC		
Rejection	entry : 1 4172 ± 4171	entry : 1 12258 ± 12257	entry : 12 1603 ± 463

Table 2: Single beam background bifurcation study (Rejection branch)
Symmetric errors are put in the rejection for your reference, however, in an actual case, this must be asymmetric.

phase space cut is imposed to avoid $K_{\pi 2}$ kinematics region, this is because, dominant component is not yet single beam backgrounds but still $K_{\pi 2}$ only with the B4ABM, which screw-ups the correct rejection measurement. So, for further enhancement of beam background events, the PNN1BOX cuts are applied. Here we assume the rejection to the beam backgrounds in the PNN1BOX is same as that of backgrounds in the KP2BOX. And then, DELC rejection is measured with tree different type of additional cuts; “TD*KIN”, “TD only”, “no additional cut”. Theoretically we should take the number of “TD*KIN”, however it has a big statistical error, we choose rather conservative value of 1603 ± 463 from loose setup cuts.

Normalization factor $N_{nomalize}$ is measured as in the table-3. All cuts are simply imposed except for inverted DELC. The obtained number is 30. Combining both branches, # of beam backgrounds is 1.87 ± 10^{-2} (= 30. / 1603.).

The number of double beam backgrounds in the signal box Single beam backgrounds are found to be suppressed well by DELC design as shown in the previous paragraph, however, if two incident particles come in, the DELC might be fooled because the possibility that the first particle makes “tk” time (, then missed) and the second particle makes “trs” time. For the rejection of this kind of events, another cuts are required to be made for the confirmation the entering particle is surely one. Watching out beam wire and Cerenkov activities around trs time

Description	PNN1 PASS1 prescale 3	
Kin, TD, PV setup cuts	KP2BOX, UTCQUAL, RNGMOM, COS3D, LAYV14, ZFRF, ZUTOUT, PV (no TGPV)	
Beam related setup cuts	TGQUALT, TGZFOOL, TARGF, DTGTTP, RTDIF, DRP, KIC, B4DEDX, BWTRS, B4ETCON, B4TRS, B4CCD, B4EKZ, TIMCON, TGTCON, TIC entry : 5253	
Anti-Tag	$\overline{\text{DELC}}$ entry : 2862	
Make branches	[Kaon beam] CPITRS, CPITAIL entry : 432	[Pion beam] CKTRS, CKTAIL entry : 2499
All other cuts	B4DEDX, KIN, TD, PV, CKTRS, CKTAIL entry : 30	B4DEDX, KIN, TD, PV, CPITRS, CPITAIL entry : 30

Table 3: Single beam background bifurcation study (Normalization branch)

is one way to kill the events, so BWTRS, CKTRS, CKTAIL, CPITRS, CPITAIL (and B4TRS, B4CCD) are designed for it.

Their rejection and # of backgrounds surviving through the cuts are measured in the same way as the previous case with a bifurcation method. For a correct rejection measurement, all event topology cuts in the target are removed from the setup in the rejection branch as summarized in the table-4. Again, to enhance the backgrounds she/he wants to measure, the two beam backgrounds are tagged with requirements of B4 activity ($\overline{\text{B4TRS,B4CCD}}$) around "trs" time. Then, the beam wire and Cerenkov (BWTRS, CKTRS, CKTAIL, CPITRS, CPITAIL) cuts are imposed and the rejections are measured. In this analysis, two branches are made depending on the second particle type.

- Additional Kaon entering events : Firstly, for the confirmation this is not pion entering events, CPITRS, CPITAIL are imposed in advance and B4 energy deposit is required to be Kaon like, namely, B4ARS > 1.1. Then, the rejection of "BWTRS, CKTRS, CKTAIL" is measured. The Kaon beam background is 1.26 (= 67/53).

- Additional pion entering events : CKTRS, CKTAIL for confirmation of no Kaon entering, and pion like dE/dX (B4ARS < 1.1) are required beforehand. Then, "BWTRS, CPITRS, CPITAIL" are imposed. The pion beam background is 6.74×10^{-2} (= 304/4512).

Description	PNN1 PASS1 prescale 3	
Kin, TD, PV setup cuts	UTCQUAL, RNGMOM, COS3D, LAYV14, ZFRF, ZUTOUT, PV (no TGPV), TD	
Beam related setup cuts	TGQUALT, TGZFOOL, DELC, B4DEDX, B4ETCON, TIMCON entry : 122126	
Two beam tag	$\overline{\text{B4TRS,B4CCD}}$, PNN1BOX entry : 16245	
Make branches	[Kaon beam] CPITRS, CPITAIL entry : 430	[Pion beam] CKTRS, CKTAIL entry : 15241
Further cuts	$1.1 <$ B4ARS < 5.0 entry : 264	B4ARS $< 1.1, TGZ > -7.0$ entry : 9023
Rejection	BWTRS, CKTRS, CKTAIL entry : 5 53 ± 23	BWTRS, CPITRS, CPITAIL entry : 2 4512 ± 3190

Table 4: Two beam background bifurcation study (Rejection branch)

3.1.2 Muon background suppression

There are some Kaon decays whose final products are muon + “something” which involve no photon or only one photon, for example, $K^+ \to \mu^+\nu$, $K^+ \to \mu^+\nu\gamma$. Such events must be well controlled by the setup cuts since they have no photon rejection or smaller rejection than the two photon (π^0) case and become background candidates. π^+ decay sequence cut, dE/dX cut in RS, phase space cuts will work for their rejection.

The table-6 shows the bifurcation study of the muon backgrounds. First of all, in order to suppress the backgrounds other than muon related one, all beam background cuts are imposed as a setup. Then, in the rejection branch, muon events are tagged with RS dE/dX cut ($\overline{\text{RSDEDX}}$) and phase space cuts; $231 < ptot < 250, rtot < 45$ for muon band selection, $190 < ptot < 231, rtot < 45, 3. < rngmon\_new3 < 10.$ for muon range tail selection. ($K_{\mu 2}$ peak events are not used for this study.) TD rejection to them is measured and the obtained number is 1059 ± 204. In the normalization branch, all cuts are imposed with reversed TD and the surviving events are counted. Combining both branches, the expected number of muon backgrounds is = 1.24×10^{-1} (= 131/1059).

Description	PNN1 PASS1 prescale 3	
Kin, TD, PV setup cuts	KP2BOX, UTCQUAL, RNGMOM, COS3D, LAYV14, ZFRF, ZUTOUT, PV (no TGPV)	
Beam related setup cuts	TGQUALT, TGZFOOL, TARGF, DTGTTP, RTDIF, DRP, DELC, KIC, B4DEDX, B4ETCON, B4EKZ, TIMCON, TGTCON, TIC entry : 8358	
Make branches	[Kaon beam] CPITRS, CPITAIL entry : 3544	[Pion beam] CKTRS, CKTAIL entry : 7664
Anti-Tag	$\overline{\text{BWTRS, CKTRS, CKTAIL}}$ entry : 511	$\overline{\text{BWTRS, CPITRS, CPITAIL}}$ entry : 4631
All other cuts	B4TRS, B4CCD, KIN, TD, PV	
	entry : 67	entry : 304

Table 5: Two beam background bifurcation study (Normalization branch)

3.1.3 The number of expected backgrounds in 1/3 sample

Now, all background estimation other than $\pi^0 \to \gamma\gamma$ background appearing through detector photon inefficiency are done. For the background measurement, PV of 50% acceptance is chosen, which is in the middle of PV acceptance scan range. Since we suppose there is no (or small) correlation between PV and other cuts, the beam backgrounds and photon disassociate muon backgrounds becomes x2/5 (= 20/50) at 20% PV acceptance position and x2 (=100/50) at 100 % PV acceptance point. As a conclution, 1.4 backgrounds are expected in 1/3 sample at 50% PV acceptance point. The results are summarized in the table-7. This can be said backgrounds are well suppressed in the case that more than 10 events are remained in the final box.

3.2 Online photon veto rejection

Now, all (or almost all) the remaining events are regarded to be $K_{\pi2}$ decays, so preparations for a photon veto measurement is done. E949 Photon veto consists of two stage, online photon veto which is implemented by hardwares and offline photon veto, software based one. Online components in the trigger are HEX, HEX afterburner, BV, BL and EC.

Description	PNN1 PASS1 prescale 3	
Kin setup cuts	UTCQUAL, COS3D, LAYV14, ZFRF, ZUTOUT, PR_RF, PR_RF_XY, PR_RFZ1, PR_RFZ2, PV	
Beam related setup cuts	TGQUALT, TGZFOOL, TARGF, DTGTTP, RTDIF, DRP, DELC, KIC, B4DEDX, BWTRS, B4ETCON, B4TRS, B4CCD, CPITRS, CPITAIL, CKTRS, CKTAIL, B4EKZ, TIMCON, TGTCON, TIC entry : 50946	
Make branches	[Rejection branch]	[Normalization branch]
Further setup	$\overline{\text{RSDEDX}}$ Muon band : $231 < ptot < 250, rtot < 45$ Range tail : $190 < ptot < 231, rtot < 45$ $3. < rngmon\_new3 < 10.$ entry : 28597	PV, KP2BOX entry : 478
Rejection — Inversion	TD entry : 27	$\overline{\text{TD}}$ entry : 169
	1059 ± 204	KIN entry : 131

Table 6: $K_{\mu 2}$, μ background bifurcation study

Online rejection is measured by two different ways. One is a way to reproduce the pnn1 data by adding photon veto trigger bits to $K_{\pi 2}(1)$ which are enough purified with tight $K_{\pi 2}$ selection cuts as mentioned in the previous section and count the remaining events. This method is robust, however, the measurement is needed to run with short statistics and is suffered from a large statistical error. One another way is to take a trigger ratio of Pnn1 over $K_{\pi 2}(1)$, where again, $K_{\pi 2}$ events should be cleanly selected with setup in the both samples, and for the $K_{\pi 2}(1)$ sample, there is one more requirement that all pnn1 online trigger bits except for photo veto must be imposed additionally. So, their difference is now PV related triggers only. In this method, there is no need to impose online photon veto triggers (whose reduction factor is, say, around 10^4) and better statistical accuracy can be expected. But prescale factors at data acquisition must be made clear, which means it requires the confirmation of no trigger loss and all events are certainly collected and recorded into a data storage.

The table-8, 9 are the rejection numbers measured by the first method. One thing to be noted here is that HEX afterburner is included in L1.2 trigger and there is no way to isolate the contribution, so, its rejection is simulated with the recorded online bits and the algorithm is mimicked by software. After the HEX afterburner cut, L1.2 still shows some rejection. That

Background type	Subcategory	# of events
Beam background	single beam	1.87×10^{-2}
	double beam (kaon entering)	1.26
	double beam (pion entering)	6.74×10^{-2}
Muon background	—-	1.24×10^{-1}
Total		1.47

Table 7: # of backgrounds in 1/3 sample

Cut name	Description	# events	Rejection
$K_{\pi 2}(1)$ raw events			
+ Setup cuts	(seen in the table-1)	36680	
+ HEX	lhex	12194	3.008 ± 0.022
+ HEX afterburner	*included in L1.2. No corresponding trigger bit.*	10986	1.110 ± 0.003
+ L1.2	l12	10491	(1.047 ± 0.002)
			3.339 ± 0.027

Table 8: Online Photon Veto Rejection (HEX and HEX-afterburner)

contribution comes from "RSHEX+" trigger bits, and which rejection is measured 1.047 ± 0.002 as seen in the table-8. This number will be used as a correction factor in the later study, however, the rejection is not so high since tighter offline π^+ quality cuts are already applied. On the other hand, EC, BV, BVL rejections are measured with $K_{\pi 2}(2)$ sample to gain more statistics. The rejection is listed in the table-9. Combining both gives us the total online rejection of 6060 ± 663.

In the same way, the table-10 shows the total online rejection measured by the second method. Comparing both results, their discrepancy is comparable with their statistical errors and it can be said both are consistent. We take the latter number of 6613 ± 35 as official. One thing to be noted here is the rejection strongly depends on the beam background cuts. In this analysis, the cuts listed in the table-1 are used for the measurement, but if the standard PNN1 beam cuts "PSCUT02" are used, the rejection gets larger as written in the table-11, 12 the total rejection become $(0.916 \pm 0.107) \times 10^4$, $(1.043 \pm 0.011) \times 10^4$ respectively. This is because some cuts in the PSCUT02 work as a target photon veto (, and also as an upstream photon veto, a ring photon veto and an I-counter photon veto). These components are not included in the online photon veto, that is why, in principle, the events making energy deposit in these subsystem survive, but the PV components in the PSCUT02 helps to remove them and this makes the rejection higher. Of course, as one can easily imagine, total rejection doesn't become larger, on the contrary, gets smaller because the rejection is taken away by PSCUT02.

Cut name	Description	# events	Rejection
	— All setup cuts —	176098	
$\overline{BV \cdot BL \cdot EC}$	$\overline{ext(4)ext(5)ext(6)}$	97	1815 ± 184

Table 9: Online Photon Veto Rejection (BV,BVL and EC)

Event type	Selection cut	# events	#events $\times$ prescale
$K_{\pi 2}(1)$	$K_{\pi 2}$ purification cuts and all pnn1 trigger bits other than PV	36680	0.4725×10^{10}
$Pnn1$	$K_{\pi 2}$ purification cuts	714509	0.7145×10^{6}
	Trigger ratio : $\frac{N(Pnn1)}{N(K_{\pi 2}(1)}$		6613 ± 35

Table 10: Online Photon Veto Rejection (by trigger ratio method)

3.3 Online photon veto acceptance

Acceptance loss by photon veto is measured with $K^+ \rightarrow \mu^+\nu_\mu$ sample, which ideally doesn't have any photon activity and the event topology is alike to the signal, *i*.e. two body decay and having one charged track.

Since our explorable acceptance region is from 10% to 100%, keeping a background level below 10^{-3} is quite enough for the measurement when obtaining it with two significant figures. π^+, μ^+ identification with a dE/dX cut and a range momentum cut can well suppress π^+ backgrounds together with a KM2BOX. Photon associate μ^+ backgrounds such as $K^+ \rightarrow \mu^+\pi^0\nu$, $\mu^+\nu\gamma$ whose branching ratio is 3.27% and 0.5% respectively can be suppressed to below the level by KM2BOX and one or two order smaller their branching ratio's than that of $K_{\mu 2}$.

3.3.1 $K_{\mu 2}$ sample selection criteria

- $K_{\mu 2}(1)$ online trigger : $K_B \cdot T2 \cdot (6_{ct} + 7_{ct}) \cdot (17_{ct} + 18_{ct} + 19_{ct})$
- offline trigger : summarized in the table-13.

There appears a noticeable difficulty in the acceptance measurement from removal of range stack counters layer 20 and 21, which causes most of μ^+s from $K_{\mu 2}$ reach to BVL and fire the ext(6) trigger bit, consequently, we have lost a traditional (and a direct) way of the acceptance measurement used in E787. In E949, we have developed two different methods and they are supplementary used because each has advantage(s) / disadvantage(s) to the other, and aim to get more confidence by confirming both give consistent results.

Cut name	Description	# events	Rejection
Run range	run > 48003 (Mean-Timer events only)		
Bad Run cuts	bad_run.f (removes CsI HV off runs)		
PASS1, KP2BOX	BAD_STC, RD_TRK, TRKTIM, UTC, RANGE1, TARGET, STLAY, TDCUT, KP2BOX		
Kinematics cuts	kincut02_nobox		
Piscat cuts	**pscut02**		
e^+ time veto	elveto_new02		
	— All setup cuts —	268488	
EC	ext(5)	165443	1.623±0.002
BV	ext(4)	906	182.6±6.1
BVL	ext(6)	97	9.340±0.896
L20ct+L21ct	lct(20).or.lct(21)	97	1.
			2768 ± 281

Table 11: Online Photon Veto Rejection (BV,BVL and EC) with PSCUT02

Event type	Selection cut (**w/ pscut02**)	# events	#events × prescale
$K_{\pi 2}(1)$	$K_{\pi 2}$ purification cuts and all pnn1 trigger bits other than PV	7990	1.034×10^9
$Pnn1$	$K_{\pi 2}$ purification cuts	99130	0.991×10^5
	Trigger ratio : $\frac{N(Pnn1)}{N(K_{\pi 2}(1))}$		$(1.043 \pm 0.011) \times 10^4$

Table 12: Online Photon Veto Rejection (by trigger ratio method) with PSCUT02

Layer 18 method The first method, called "*l*ayer 18 method", is a way to collect short range (in RS) $K_{\mu 2}$ muons by imposing the stopping layer must be 18 or inner. The major part of the $K_{\mu 2}$s are killed by it but a portion of them having a large dip angle or longer target range survive. The advantage of the method is that online or offline acceptance can be directly measured by applying online or offline cuts and straightforwardly can count how many $K_{\mu 2}$s are vetoed.

Blankout method The other method is called "*blankout method*", which is a kind of "detector masking method", concealing all activities around a μ^+ track and measures acceptance drop only in the unmasked region. The acceptance drop in masked region is estimated from the acceptance of unmasked region by assuming accidentals distribute homogeneously. An advantage compared with the layer 18 method is, since most of $K_{\mu 2}$s get available this time, it can avoid a possible bias from the requirement of stopping layer $\leq$ 18. However, there is no way left to measure online acceptance because mostly BVL has fake photon hits by muons. But the method can measure offline acceptance, and also total acceptance in the case that the offline cuts fully

Category	Cut Entry
RUN	BAD_RUN, $run \geqq 48077$
	discard runs : $48540 \leqq run \leqq 48575$
$K_{\mu 2}$ box cuts	KM2BOX
Kinematic cuts	
	ICODEL14, UTCQUAL, RTGHI, ETGHI, PIGAP
— Fiducial —	COS3D, ZFRF, ZUTOUT
— PRRF —	PR_RF, PR_RF_XY, PR_RFZ1, PR_RFZ2
— TGLIKE —	TGLIKE1, TGLIKE2
— TGDB4 —	TGDB4, TGDB4TIP, TGDVXTIP, TGDVXPI
Beam background cuts	
	DELC, KIC
— TG pattern —	TGQUALT, TGZFOOL, TARGF, DTGTTP, RTDIF, DRP
— B4BWBH —	B4DEDX, BWTRS, B4ETCON, B4TRS, B4CCD
— Cerenkov —	CPITRS, CPITAIL, CKTRS, CKTAIL
— TG energy —	B4EKZ
— Timing —	TIMCON, TGTCON, TIC

Table 13: $K_{\mu 2}$ event purification cuts

include the online cuts.

The table-14, 15 are lists of measured acceptance by layer 18 method and blankout method respectively. They are well consistent each other except for unmeasured *blankout*ed triggers. Systemtics in both mothods are evaluated later.

3.4 Offline photon veto rejection and acceptance

Offline photon veto is designed to free from correlation to a charged track kinematics as much as possible and the algorithm is made simple to avoid possible bias because we perform an optimization later, if not simple, it may easily fall into a biased result. The algorithm is that, for each photon veto subsystem, a time offset t_{offset} and a half timing window t_{win} are fixed and all energy deposit satisfying $|t - t_{offset}| < t_{win}$ are summed up. If the energy is bigger than the given threshold $E_{threshold}$, the event is rejected.

There are a few points to be noted here, (1) we *d*on't reconstruct π^0. It is true if the π^0 reconstruction done, it would be free from acceptance loss and would become more effective cut, however it is critical if one of π^0 origin photons escapes to a beam line direction. Photon rejection we need is much severe than it. (2) we *d*on't use charge track information to avoid bias, as already mentioned.

Cut name	Description	# events	Acceptance
	— All setup cuts —	15183	
HEX	lhex	14168	0.933±0.002
HEX afterburner	*included in L1.2. No corresponding trigger bit.*	13869	0.979±0.001
EC	ext(5)	13711	0.987±0.001
BV	ext(4)	13562	0.989±0.001
BVL	ext(6)	13308	0.978±0.001
L20ct+L21ct	lct(20).or.lct(21)	13220	0.993±0.001
Online total			0.871±0.003

Table 14: Online Photon Veto Acceptance (Layer18 method)

Cut name	Description	# events	Acceptance
	— All setup cuts —	113400	
HEX	lhex	106159	0.936±0.001
HEX afterburner	*included in L1.2. No corresponding trigger bit.*	103818	0.978±0.001
EC	ext(5)	102643	0.989±0.001
BV	ext(4)	(BLANKOUTed)	—
BVL	ext(6)	(BLANKOUTed)	—
L20ct+L21ct	lct(20).or.lct(21)	(BLANKOUTed)	—
Online total		0.905±0.001 × "BLANKOUTed" factor	

Table 15: Online Photon Veto Acceptance (Blankout method)

Blind effects by early accidentals Basically for the record of the photon hit timing, multi hit TDCs are used, so, there is no problem even if more than two hits come after the TDC start gate, however, successive two pulses coming within a discriminator gate, the second one is masked by the early pulse and only the first one's timing is recorded. This kind of events are observed as an early timing hits having significant photon energy. For example, the figure-1 shows the TDC screw-upped events in BV. Their timing are significant earlier than a prompt peak, but their energy distribution looks like that of the prompt peak. The same phenomenon is seen in BVL distribution. Therefore, in BV/BVL, wide window but loose energy cuts are introduced. So, now we have 22 subsystems for offline photo veto in total.

3.4.1 Parameter scan and search for the most efficient cut set

As mentioned before, $Br(\pi^0 \to \nu\bar{\nu})$ is proportional to the inverse of "photon veto rejection" × "acceptance", thus, it is worthful to have an trial of search for the best point giving the biggest number by measuring rejection and acceptance simultaneously.

There are 22 subsystems for photon veto and they have different timing resolution, S/N ratio and so on, therefore, it is not so straightforward for finding the best set by eye scan. Here we perform an automatic optimization with a help of huge amount of CPU resources.

3.5 Total photon veto rejection vs acceptance

The figure-8 is the obtained profile curve by an automatic optimization process. The open triangle shows the π^0 rejection vs acceptance and the closed triangle is the effective rejection which is defined as rejection$\times$acceptance.

Subsystem	T_{Offset}	T_{Win}	$E_{Thr.}$
BV	5.398	9.300	0.400
BVL	1.800	1.300	0.400
early BV hit	-9.400	28.800	9.600
early BL hit	-22.600	26.400	7.300
end cap	7.255	21.900	0.109
RD	11.695	25.775	0.200
target	-0.600	2.300	1.690
I-counter	1.450	4.150	1.800
V-counter	0.650	2.500	1.200
collar	3.150	3.350	1.400
micro-collar	-1.000	3.000	0.800
EC (ring-1)	9.252	17.238	0.204
BV SAST	-10.700	9.500	1.800
RD SAST	0.400	4.800	14.000
RD SABT	1.291	23.500	0.000
RD NABT	0.750	2.000	0.400
RD BAST	11.691	10.800	9.600
BV SABT	3.700	3.000	0.000
BV NABT	0.300	2.400	4.800
BV BAST	16.100	7.200	0.300
EC (2nd pulse)	-5.300	1.200	18.600
BL BAST	-0.200	14.400	11.400

Table 16: Offline Photon Veto Cuts

3.6 The final photon veto cuts

The table-16 is the final cut parameters selected from the profile curve. A point at the acceptance of 0.1173 is chosen.

EC (ring-1) : The most inner ring of EC is treated as a separate category because of the high accidental occupancy.

BV SAST : BV category for the single end ADC and single end TDC hit.

RD SAST : A category for RD single end ADC, single end TDC hits.

◯A◯T : ‘A’ and ‘T’ means ADC and TDC. In the circle ◯, ‘B’ or ‘S’ or ‘N’ will sit. Each character is a representative of

B : Both ends

S : Single end

N : No hit

EC (2nd pulse) : EC 2nd pulse found by CCD double pulse finding is treated as a separate category.

Cut name	Normal $K_{\pi 2}$ events	$K_{\pi 2}$ events but all π^0 activities are removed
# raw generated events	2.8×10^6	2.8×10^6
$K_{\pi 2}(1)$ trigger	1036482	1007045
IC	(—)	(—)
DC	882227	852338
Level 1.n	(—)	(—)
$\overline{L0\_ZFRF}$	484895	521401
L0rr1(1)·US + L0rr1(2)·DS	477289	518411
KP2BOX	385506	446491
misc additional setup cuts	168880	262719
online photon veto	4	262715
offline photon veto	4	257715

Table 17: Reconstruction disruption factor

3.7 Measurement of the track reconstruction disruption factor C_{dis} and hidden photon veto rejection in setup

Photon activities around or right onto a π^+ track sometimes interfere a track reconstruction by making fake track counters or creating anomalous dE/dX which is likely to prevent from linking the track trajectory. The effect causes further acceptance drop during finding π^+s of $K_{\pi 2}$s, consequently, the number of π^0s in a denominator of the upper limit equation-4, gets underestimated. Even if, fortunately, the overlapping photons don't make it failure, their energy deposits are certainly contained in the measured π^+ energy and such events will be dropped at a π^+ energy selection cut. Actually, this phenomena are observed when one makes a plot of "measured π^+ momentum vs measured π^+ energy" or "measured π^+ range vs measured π^+ energy", one can see events having correct $K_{\pi 2}$ momentum, range, however, having around 20 MeV larger energy. They are the dropped shadow of $K_{\pi 2}$ events by overlapping photon.

The former case is a reconstruction disruption example and the latter case is an example that some setup cuts have photon rejection ability. There are also several known triggers or cuts unintentionally having photon rejection, since in the real world it is impossible to make an ideal cut working only for muon/beam backgrounds. The rejections are always mixed up, somehow.

Here, the disruption factor C_{dis} together with the hidden rejection in the setup cuts are measured. Note that the measurements are done at a time and there is no clear boundary between them, thus, C_{dis} is re-defined from now to include all contribution.

The table-17 is the disruption factor in the online trigger components. The measurement is purely MC based one and the method is, generating two sets of data, one is a collection of normal $K_{\pi 2}$ decays and the other is a set of cheated $K_{\pi 2}$ decays where π^0s are removed right after the kaon decay, and their acceptance numbers are compared with each other after their track reconstruction. Two information can be extracted from the table. One is the disruption factor including hidden rejection, which is $1.1582 \pm 0.0007 (= 446491/385506)$ and one another is a self veto factor, in another words, the ratio of π^+ making a real or fake photon hit. This is 0.9810 ± 0.0003 ($= 257715/262719$).

In the same way, the table-18 shows the factor in the offline components. In this measurement, piscat data are used as none photon (π^0) associate sample. In the table, "π^+ scatter-in (1)" means piscat events with KP2BOX phase space cuts, and "π^+ scatter-in (2)" means piscat with PNN1BOX cuts. As can be seen, no hidden photon veto rejection is observed. As a conclusion, C_{dis} is measured as $1.136 (= 1.1582 \times 0.9810)$.

Cut name	$K_{\pi 2}(1)$	π^+ scatter-in (1)	π^+ scatter-in (2)
run range cut	1860446 (—)	4069163 (—)	4069163 (—)
pnn1 trigger (w/o PV)	225015 (—)	(not imposed)	(not imposed)
Phase space	176530 (—)	115847 (—)	133919 (—)
DUPEV, TRBIT	(not imposed)	(not imposed)	(not imposed)
LEV11, LEV12	(not imposed)	(not imposed)	(not imposed)
RD_TRK	176530 (1.000 ± 0.000)	115847 (1.000 ± 0.000)	133919 (1.000 ± 0.000)
STLAY	175376 (1.007 ± 0.000)	108376 (1.069 ± 0.001)	126822 (1.056 ± 0.001)
BAD_STC	175376 (1.000 ± 0.000)	108018 (1.003 ± 0.000)	126726 (1.001 ± 0.000)
RSHEX	167818 (1.045 ± 0.001)	101983 (1.059 ± 0.001)	120413 (1.052 ± 0.001)
TRKTIM	167818 (1.000 ± 0.000)	101983 (1.000 ± 0.000)	120413 (1.000 ± 0.000)
UTC	167818 (1.000 ± 0.000)	101983 (1.000 ± 0.000)	120413 (1.000 ± 0.000)
RDUTM	167818 (1.000 ± 0.000)	101983 (1.000 ± 0.000)	120413 (1.000 ± 0.000)
PDC	167818 (1.000 ± 0.000)	101983 (1.000 ± 0.000)	120413 (1.000 ± 0.000)
LAY14	167812 (1.000 ± 0.000)	101960 (1.000 ± 0.000)	119258 (1.010 ± 0.000)
UTC1	167812 (1.000 ± 0.000)	101960 (1.000 ± 0.000)	119258 (1.000 ± 0.000)
RANGE1	167812 (1.000 ± 0.000)	101960 (1.000 ± 0.000)	119258 (1.000 ± 0.000)
RSHEX2	164407 (1.021 ± 0.000)	99492 (1.025 ± 0.001)	116139 (1.027 ± 0.000)
TARGET	164047 (1.002 ± 0.000)	96337 (1.033 ± 0.001)	111511 (1.042 ± 0.001)
FITPI	160067 (1.025 ± 0.000)	79100 (1.218 ± 0.002)	90009 (1.239 ± 0.002)
PSCUT (inactive)	—	—	—
TGCUT (inactive)	—	—	—
ICODL14	159774 (1.002 ± 0.000)	78962 (1.002 ± 0.000)	89428 (1.006 ± 0.000)
UTCQUAL	143874 (1.111 ± 0.001)	57503 (1.373 ± 0.003)	64842 (1.379 ± 0.003)
RNGMON	142633 (1.009 ± 0.000)	57054 (1.008 ± 0.000)	63834 (1.016 ± 0.000)
PIGAP	141465 (1.008 ± 0.000)	52630 (1.084 ± 0.001)	58841 (1.085 ± 0.001)
COS3D	140365 (1.008 ± 0.000)	51872 (1.015 ± 0.001)	58141 (1.012 ± 0.000)
LAYV4	140363 (1.000 ± 0.000)	37993 (1.365 ± 0.004)	57090 (1.018 ± 0.001)
ZFRF	135113 (1.039 ± 0.001)	36876 (1.030 ± 0.001)	53677 (1.064 ± 0.001)
ZUTOUT	135103 (1.000 ± 0.000)	36871 (1.000 ± 0.000)	53655 (1.000 ± 0.000)
RSDEDXCL	117295 (1.151 ± 0.001)	31974 (1.153 ± 0.002)	46293 (1.159 ± 0.002)
RSDEDXMAX	115815 (1.013 ± 0.000)	31563 (1.013 ± 0.001)	45596 (1.015 ± 0.001)
RSLIKE	115813 (1.000 ± 0.000)	31563 (1.000 ± 0.000)	45447 (1.003 ± 0.000)
PR_RF	112026 (1.034 ± 0.001)	30548 (1.033 ± 0.001)	42658 (1.065 ± 0.001)
PR_RF_XY	101834 (1.100 ± 0.001)	27838 (1.097 ± 0.002)	39506 (1.080 ± 0.001)
PR_RFZ1,2	92108 (1.106 ± 0.001)	25165 (1.106 ± 0.002)	34783 (1.136 ± 0.002)
TGLIKE1	89981 (1.024 ± 0.001)	23274 (1.081 ± 0.002)	32333 (1.076 ± 0.002)
TGLIKE2	89112 (1.010 ± 0.000)	22419 (1.038 ± 0.001)	31219 (1.036 ± 0.001)
TGDB4	87001 (1.024 ± 0.001)	19875 (1.128 ± 0.003)	27186 (1.148 ± 0.003)

Cut name	Description	# events	Acceptance
	pnn1 events	188588	—
HEX afterburner	(simulated)	173416	0.9195 ± 0.0006

Table 19: Additional acceptance drop by HEX afterburner simulation with recorded trigger bits

TGDB4TIP	86167 (1.010 ± 0.000)	12593 (1.578 ± 0.009)	18193 (1.494 ± 0.006)
TGDVXTIP	85587 (1.007 ± 0.000)	10621 (1.186 ± 0.005)	15437 (1.179 ± 0.004)
TGDVXPI	83696 (1.023 ± 0.001)	9814 (1.082 ± 0.003)	13838 (1.116 ± 0.003)
IPIFLG	83535 (1.002 ± 0.000)	9792 (1.002 ± 0.000)	13813 (1.002 ± 0.000)
EV5	69008 (1.211 ± 0.002)	8118 (1.206 ± 0.006)	11439 (1.208 ± 0.005)
TDFOOL	67409 (1.024 ± 0.001)	7878 (1.030 ± 0.002)	11123 (1.028 ± 0.002)
TDVARNN	55021 (1.225 ± 0.002)	5975 (1.318 ± 0.008)	8505 (1.308 ± 0.007)

Table 18: Setup cuts rejection to $K_{\pi 2}$, π^+ scatter-in events

3.8 Systematic errors in the measurements

We observed queer phenomena that some recorded trigger bits are sometimes inconsistent with the one used in actual triggers. For example, $K_{\pi 2}(2)$ trigger has a HEX in its definition, thus, ideally only one hextant or adjoining two hextants have a ".true.", but in an actual case, we observed some events having more than tree hextants have "$hhex(i) = .true.$". We believe this is just a latch timing problem or screw-ups in our monitor lines and the triggers themselves worked fine. But when we measured the rejection and acceptance, we *d*id use the trigger bits, which means the error must be included in the systematics.

Further HEX afterburner rejection is measured with pnn1 data set. Note that the HEX afterburner is a part of the pnn1 trigger, ideally no rejection can be seen, so the observed further rejection fully comes from its error. The result is summarized in the table-19, in which 8% error is measured. Unfortunately, there is no way of measuring the counterpart case, namely, actual trigger says "HEX-afterburner failed" but the recorded bits say "it passed.".

The same things are observed in the $\overline{\text{l0\_zrfrf}}$ trigger bit (described by the equation-8) as shown in the table-20. Additional 0.5% rejection is found in it.

$$\overline{\text{l0\_zfrf}} \equiv \text{.not.}(lct(13)\text{.and.}lct(14)\text{.and..not.}lct(15)\text{.and.}ext(14)) \quad (8)$$

So, as a conclusion, we add 8.5% (=8.0+0.5) error for the measured rejection and 2.2% for the acceptance. (because acceptance drop by HEX afterburner is 2.2%, the error is limitted to the number.)

Cut name	Description	# events	Acceptance
	pnn1 events	188588	—
$\overline{\text{l0\_zfrf}}$	(ref. the equation-8)	187704	0.9953 ± 0.0002

Table 20: Additional acceptance drop by recorded $\overline{\text{l0\_zfrf}}$

3.9 Result — 1/3 sample

After opening the signal box with 1/3 sample, 20 events are observed. By following Poisson statistics, N_{90} is equal to 28 in the case of 20 events observation. And the total number of π^0 used in this analysis is $1564739136 (= 1.5647 \times 10^9)$.

Therefore, the upper limit is calculated as

$$\begin{aligned} Br &< \frac{28}{1.5647 \times 10^9} \frac{1.}{1.136 \times 0.1173} && (9) \\ &< 1.34 \times 10^{-7} && (10) \end{aligned}$$

This is the 1/3 based upper limit of this mode. Because, the PV cut tuning was done with this 1/3 sample, naturally, the result is biased somehow. (Perhaps, 20 remaining events are too small, the bias may become big.)

4 Single Photon Inefficiency Study

4.1 Motivation and goal

Since the very dominant background in this decay mode is $\pi^0 \to \gamma\gamma$, (π^0 decaying into two photons and then their photons are missed in some mechanism), understanding their contamination from the view of photon inefficiency is a crucial issue for the analysis. There are several known mechanisms causing the inefficiency; dead material, detector hole, lack of radiation length, sampling fluctuation, photo-nuclear interaction and so on. Some are well studied and the contribution is well understood, but some are not. The goal of this study is to make their contribution clear as much as possible with an actual data / detector and to try to subtract backgrounds quite confidently rather than Monte Carlo based estimation. Making the goal more elaborating;

- Where do the backgrounds come from ? Get information about their mechanism, geometrical distribution and so on. If the energy dependent inefficiency is measured, contributions from photo-nuclear interaction and/or sampling fluctuation can be discussed. Also if geometrical dependency is measured, dead matrial effect and inefficiency from a beam hole can be revealed.
- How much are they ? This is the most important issue for the background subtraction. If the measurement is done with small uncertainty, we can reliably subtract them from the surviving events in the final box and this is directly connected to the improvement of the upper limit.
- Any significant signature which helps a discrimination of signals form the backgrounds ? If the inefficiency has a dependency to the geometry, π^0 rejection varies depending on its flight direction, and the effect appears as a distortion in the tagging side π^+ distribution of surviving events.
- Any technical way to kill the backgrounds more effectively. Because we make clear the inefficiency mechanism, there is a chance to invent a better cut against the inefficiency part.
- Any possible feedback for next coming experiments.

4.2 A basic idea and an analysis strategy

Beacuse E949 is a stopped Kaon experiment, even if one particle is undetected, we can determine the kinematics of the missing particle by measuring all other final products. Collecting one photon missing $K_{\pi 2}$ events tells us how often a photon is missed with determining its flight direction and energy event-by-event. This means we have a tool to make a photon inefficiency map as a function of detector geometry and photon energy.

Analysis strategy Firstly, $K_{\pi 2}$ normal photon distribution is required to be measured with the trigger constraints that π^+ goes into detector acceptance. The measured distribution; # of photons as a function of energy and the flight direction is named as a *"SPI denominator map"* and denoted as $N^{\text{denom}}(\theta, E)$. Next, in the same way, # of mis-detected photons vs their energy and the flight direction is measured, which is named as *"SPI numerator map"*, and written as $N^{\text{numer}}(\theta, E)$. By introducing a proper normalization factor A_{norm}, the single photon inefficiency table is obtained by

$$\frac{N^{\text{numer}}(\theta, E)}{N^{\text{denom}}(\theta, E)} \times A_{\text{norm}} \tag{11}$$

where θ is a polar angle in the detector geometry. Note that ϕ angle is ignored because our detector is designed in a homogeneously way along ϕ direction. (add a figure showing detector geometry and axis.)

4.3 Trigger and data set

By following the above strategy, two set of data are prepared in this analysis. One is a $K_{\pi 2}(1)$ data set defined as the equation-12. The sample doesn't have photon veto component in the trigger, so, it is proper for the denominator map measurement. The other sample is called as 1gamma data set defined by the equation-13, whose base is basically $K_{\pi 2}(1)$ but having further conditions; 'BV' is a single photon requirement in barrel region and "$\overline{NG2} \cdot HEX \cdot L1.2 \cdot \overline{EC}$" is a 2nd photon veto to confirm one photon is certainly missed.

$$K_{\pi 2}(1) \equiv K_B \cdot T2 \cdot (6_{ct} + 7_{ct}) \cdot \overline{19_{ct}} \tag{12}$$

$$1gamma \equiv K_{\pi 2}(1) \cdot IC \cdot DC \cdot L1.1 \cdot BV \cdot \overline{NG2} \cdot HEX \cdot L1.2 \cdot \overline{EC} \tag{13}$$

Data size 1gamma data with the above trigger condition were collected through run-47592 to run-48975 and totally we have 1.7×10^6 raw events.

But as shown in the table-21, there were some modifications/glitches related to photon vetoes in some runs, some are problematic for this study and needed to be removed, so, runs before run-40877 are discarded and the remaining data are decided to be used for this analysis. 14 % of the events will be lost by this run range cut.

4.4 Event purification and setup cut design

In order to purify both samples further, offline cuts are additionally imposed. Before moving into the cut list, let us clear the requirement on the purification. Single photon inefficiency is expected to vary from $10^{-2} \sim 10^{-4}$ level, therefore, backgrounds must be controlled down to the 10^{-5} level. Fortunately, one benefit of this study is no longer bothered by single π^+ scatter-in backgrounds thanks to the one photon requirement in BV. So, the dominant background type

Run range	Description
47592 $\sim$ 47719	ASUM
48003 $\sim$ 48975	MT
47592 $\sim$ 48002	BV NG2
48003 $\sim$ 48975	BV NG2
47592 $\sim$ 48076	L1.2 broken
48077 $\sim$ 48134	L1.2 Not fully functioning
47592 $\sim$ 48231	EC CFD unplugged.

Table 21: Available run range for single photon inefficiency study

gets changed from the one in the upper limit analysis. This is a great advantage for reliable measurement. Obviously, $K^+ \to \mu^+\nu\gamma$ or $K^+ \to \mu^+\nu$ + (accidental) become background candidates, this time. That is why, π^+-μ^+ identification by tracing π^+ decay sequence and dE/dX cut must be carefully designed. The table-22 is the whole set of cuts with showing how the acceptance drops through the cuts.

One comment on the daliz decay $\pi^0 \to \gamma e^+e^-$ must be mentioned here. Since the mode has one photon essentially, which matches to the 1gamma trigger condition, and worse thing, missing photon kinematics is wrongly reconstructed when the $\pi^0 \to \gamma\gamma$ assumption is used. But that case actually never happens because they are always vetoed due to their footprint in the active scintillator target (, since they are charged particles). That is why they are vetoed by the 2nd photon rejection even if the $e^{+/-}$ flight toward a beam line hole. Quantatively speaking, the numerator map is never smeared by them, and the denominator is smeared at 1% level, infered from Br($\pi^0 \to \gamma e^+e^-$) / Br($\pi^0 \to \gamma\gamma$).

4.5 Photon reconstruction — clustering algorithm

Before everything, it is necessary to retrieve photon kinematic information by properly collecting the energy deposits spread in the detector. A photon energy clustering algorithm is developed for the sake of it. The clustering techniques are summarized as follows.

1. A cluster core is searched through all barrel modules. Here, the most energetic one is assigned to the core.

2. A cone; whose angle is 25 degree is defined by assigning the cone vertex to a Kaon decay position and the base center to the cluster core as shown in the figure-(). Since the minimum opening angle of π^0 two photons is 60 degree in the Kaon rest system, if more

Cut names	Description	#events	#events in $K_{\pi 2}$ box
misc. online trigger	IC*DC*L1.1		
Fiducial	abs(cos3d)<0.5,		
	8<=layv4<=16		
Target reconstruction	itgqualt<=1		
Strobe timing	abs(tk-b4strobe)<3.7,		
	abs(tpi-trs)<5.4		
Kaon decay position	tgz>-15		
Gap btwn K^+, π^+ fiber	dist_targf<1.5		
I-counter hit time	ictime-trs+0.56<3		
TG, DC track matching	abs(dttg_tp)<2		
TD cut	ipiflg.eq.0		
B4 dE/dX	b4abm_atc>1.1		
Kaon decay time	tpi-tk>2.0		
Cerenkov TRS time veto	abs(cktrs)>1.154,		
	abs(cpitrs)>4.25		
Beam wire TRS time veto	abs(bw1trs)>1.87,		
	abs(bw2trs)>1.33		
B4 TRS time veto	abs(b4str)>2.98 when		
	b4tbm>10		
KPI2BOX	cut(26)		

Table 22: Available run range for single photon inefficiency study

larger cone angle is selected, for example, 30 degree = (60./2), one cluster cone starts eating the other photon energy deposit.

3. All photon activities inside the cone are collected if the timing is in the window of $\pm$3ns from the cluster core time.

4. By summing up their energy with taking into account the visible fraction for every subsystem, photo energy is reconstructed. Their flight direction and timing are decided by the energy weighted mean.

5. Iterations will be done. After the cone is refined with the reconstructed information and the above processes are repeated again.

4.5.1 Photon reconstruction performance

Clustering performance is checked with MC data. Their residual distributions are plotted in the figure-() and the resolutions are summarized in the table-23. Taking the ϕ resolution as an

	Resolution (radian)
θ direction	0.028
ϕ direction	0.038

Table 23: Cluster reconstruction resolution (MC)

example, that resolution is better than one third of a BV single rod (0.0436=$2\pi/48$modules$/3$) and slightly worse than quarter of the rod (0.0327=$2\pi/48$modules$/4$).

4.6 Tagging photon selection criteria

Tagging photon selection is quite important for this study since the kinematics is directly reflected to the missing side photon kinematics. As mentioned, single photon inefficiency varies $10^{-2} \sim 10^{-4}$. If a wrongly measured tagging photon exists and a cross talk happens for example from a 10^{-2} cell to a 10^{-4} cell in the worst case, it terribly screw-ups the SPI measurement. This cross talk can be removed more or less by a smearing estimation matrix from MC, however it is needed to be suppressed as much as possible by a design of tagging photon selection.

Here is a list of selection criteria;

1. Timing cuts: The hit time must be in (-3ns,3ns) around “trs”.
2. Energy cuts: More than 15 MeV is required.
   Minimum photon energy from $K_{\pi2}$ neutral pion is $\sim$ 20 MeV. “15” means energy resolution is a little taken into account.
3. Fiducial cuts: In order to confirm all energy is safely included in the detector, a few additional requirements are imposed;
   (a) Conversion position : conversion must start from an inner position of the photon detector. Energy deposit in “BL and BV-layer1” must be $>$ 10 MeV.
   (b) Photon flight direction : the dip angle (, denoted as $|sin(\theta)|$) must be $<$ 0.45. There exists a thin radiation-length area around the boundary of barrel and end cap.
   (c) Overlapping cuts : Photon flight direction must be well apart from the charged track trajectory. As shown in the figure-(), it must be 4 sector away from the track in an anticlockwise direction, and 2 sector away in a clockwise direction.

4.7 $K_{\pi2}$ event reconstruction and missing photon kinematics

To obtain missing photon kinematics, $K_{\pi2}$ event reconstruction is performed. There exists one relation between the tagging photon and π^+ kinematics *i.e.* the tagging photon energy in the lab system is uniquely decided as a function of opening angle from the π^0 boost direction because the photon energy in the π^0 CM system is monochromatic and also π^0 energy in the lab system is monochromatic. This will works as selection cuts for the wrongly measured tagging photons. There are also another constraints that the combined momentum vector should be 0 since they come from a stopped K^+. The event reconstruction is required to satisfy these constraints, here, Lagrange multiplier method is employed, which is suited for the fitting involuving some constrains.

4.7.1 Kinematical fit with Lagrange multiplier

Lagrange multiplier is a method to minimize a chi square defined as the equation-14 while keeping the given set of constraints. It takes some measured values and their resolution as inputs and returns the best fit for them and the best estimation for unmeasured values through the constraints. The event reconstruction goodness can be obtained from the chi square probability.

$$\chi^2 = \Sigma \left(\frac{X_{measured,i} - X_{fit,i}}{\sigma_i} \right)^2 \tag{14}$$

For some measured values, it is difficult to measure their resolution only with the real data since the measurements need ideal references, thus, firstly the same analysis is worked out with MC data set and later, with an assumption that MC data is not so far from the real world, real data based analysis is performed with an extrapolated resolution from the MC. This extrapolation is carried out by "stretch function", which will be mentioned later.

4.7.2 Event reconstruction with MC data set

Input variables The table-24 is a list of the input variables and their resolution directly obtained from MC data. Flight direction of π^+ ($cos3d$, $phi0$) and tagging photon (θ_{tag}, ϕ_{tag}) and its energy E_{tag}, totally five variables are used as inputs. Note that, since we know an ideal π^+ momentum, the ideal constant is used rather than the measured one.

Constraints There are four constraints; three are from momentum conservation requiring the combined momentum must be equal to the parent K^+ momentum, namely zero. The other one is the constraint to confirm the tagging photon surely comes from π^0. In another words, π^0 mass is obtained if an invariant mass is constructed with the tagging photon and the missing photon.

$$\Sigma P_x^i = 0, \qquad \Sigma P_y^i = 0, \qquad \Sigma P_z^i = 0 \tag{15}$$

$$M_{\gamma_1\gamma_2} = m_{\pi^0} \tag{16}$$

Name	Variable	Resolution
π^+ Kinematics		
Momentum	(ideal number)	(—)
Dip angle	cos3d	0.0291 [rad.]
ϕ angle	phi0	0.0283 [rad.]
Tagging photon kinematics		
Energy	E_{tag}	1.83 × sqrt(E_{tag}) [MeV]
θ angle	θ_{tag}	0.0283 [rad.]
ϕ angle	ϕ_{tag}	0.0388 [rad.]

Table 24: Input variables for Kinematical fit (MC)

Fitting performance and the missing photon kinematics table and basic resolution and improvement resolution of missing photon kinematics. reconstruction quality (chi square)

Stretch functions Stretch function is the function defined as the equation-17, which will be a normal gaussian $N(0, 1)$ if the $X_{measured,i}$ and $\sigma_{measured,i}$ are correctly measured. Basically two information can be extracted from the shape of the stretch function; peak offset gives us a information about the rightness of the $X_{measured,i}$ measurement, for example, $X_{measured,i}$ always shifts to bigger/smaller number (and other $X_{measured,j}$ are properly measured), the offset appears as a peak shift of the stretch function. The other is the shape width of the function, namely if the $\sigma_{measured,i}$ is overestimated/underestimated, the width gets narrow/wide. Of course, other distortion in the function shape tells us more information because that is a sign a certain miss-measurement appears through a functional correlation. But, it is difficult to extract straightforwardly what is wrong or how much wrong.

$$\frac{X_{measured,i} - X_{fit,i}}{\sqrt{\sigma^2_{measured,i} - \sigma^2_{fit,i}}} \tag{17}$$

For an estimation of the unknown $\sigma_{measured,i}$s in real data, firstly, using the MC $\sigma_{measured,i}$s but with "real data" $X_{measured,i}$, the stretch function is plotted for each measured variables. After confirming the peak is standing at 0 and the shape is gaussian like, defining $\sigma^{real}_{measured,i} \equiv \sqrt{C_i} \times \sigma^{umc}_{measured,i}$, where $\sigma^{real}_{measured,i}$ is a measured resolution of real data, and $\sigma^{umc}_{measured,i}$ is that of MC, the best $\sigma^{real}_{measured,i}$ is scanned by changing C_i. The obtained $\sigma_{measured,i}$ for real data is shown in the table-25.

Reconstruction quality Now all required information is prepared. Above mentioned process is redone with real data, and the figure-() is the chi square probability distribution. Event reconstruction works fine as seen in the plot, the nice flatness is obtained. To robustly discard

Name	Variable	Resolution
π^+ Kinematics		
Momentum	(ideal number)	(—)
Dip angle	cos3d	0.034 [rad.]
ϕ angle	phi0	0.035 [rad.]
Tagging photon kinematics		
Energy	E_{tag}	2.12×sqrt(E_{tag}) [MeV]
θ angle	θ_{tag}	0.033 [rad.]
ϕ angle	ϕ_{tag}	0.046 [rad.]

Table 25: Input variables for Kinematical fit (Real data)

the wrongly reconstructed events, cut position is chosen that the chi square probability must be larger than 0.2.

4.8 Denominator Map

Denominator map is measured with $K_{\pi 2}(1)$ events imposing $K_{\pi 2}$ event purification, photon reconstruction cut, tagging photon section, $K_{\pi 2}$ event reconstruction and its chi square quality cut. The table-() is the map.

4.9 Numerator map

For numerator map, 1gamma data set is used, however, setup cuts and all reconstructions must be done in the exactly same way. Only one difference is, offline 2nd photon veto is imposed further from now. Offline 2nd photon consists of two process, one is remove of the tagging photon. Temporary all energy deposit belonging to the tagging photon is put away from hit entry banks. The other is the offline photo veto obtained from the parameter scan in the section-(), these offline cuts are additionally imposed to the 1gamma data set and # of surviving entry is counted for each E, θ bin. In the former process, occasionally tagging photo split into more than two clusters in the conversion stage. This may cause the self veto, so, the effect is studied later.

The table-(,,,) is the obtained numerator maps for each photo veto cuts.

4.10 Normalization factor

Since the trigger prescale factors are different between those two data set, when taking a ratio of $N^{numer}(\theta, E)$ over $N^{denom}(\theta, E)$, a normalization factor A_{norm} is required. The normalization factor can be measured by reproducing the 1gamma data set from the $K_{\pi 2}(1)$ data set and taking

	Real $K_{\pi 2}(1)$ data set (SPI analysis run range)	Real $K_{\pi 2}(1)$ data set (whole run range)	MC $K_{\pi 2}$ data set
raw events	45985	184275	780598
Tagging photon selection	34885	140063	621431
(acceptance)	0.759 ± 0.002	0.760 ± 0.001	0.796 ± 0.001
Event recon. chi square cut	24946	101119	493312
(acceptance)	0.715 ± 0.002	0.722 ± 0.001	0.743 ± 0.001
Online 2nd photon PV	2047	9117	—
(acceptance)	0.082 ± 0.002	0.090 ± 0.001	—
(rejection)	12.19 ± 0.26	11.09 ± 0.08	—

Table 26: 1gamma trigger simulation to $K_{\pi 2}(1)$ data set

a ratio between the # of 1gamma data set and the # of reproduced 1gamma data set. The table-26 is the number of 1gamma events in the $K_{\pi 2}(1)$ data set. For convenience, tagging photon selection and event reconstruction cut are imposed as setup cuts. Now, there are 580389 1gamm trigger events we have after tagging photon selection and event reconstruction cut. Thus, the normalization factor A_{norm} is 63.66 ± 0.66 (= 580380 / 9117).

4.11 Correction factors

There are three correction factors must be taken into account. One is a "RSHEX+" component in L1.2 trigger bit. The L1.2 consists of "HEX afterburner" and "RSHEX+", hence the HEX afterburner works as photon veto, the trigger bit is included in the online 2nd photon veto component. But RSHEX+ is a charged track related trigger, so that, the contribution must be removed.

RSHEX+ rejection in L1.2 The RSHEX+ rejection is measured with $K_{\pi 2}(1)$ data set. Firstly, all required setup cuts are imposed to the sample, and then, 1gamma trigger bits excluding L1.2 are imposed further. The entries can be seen in the table-27. After counting the # of remaining events, HEX afterburner cut is applied, as shown in the table, 4382 events are surviving. Then, the L1.2 trigger bit is imposed. Because HEX afterburner is already imposed, no rejection is seen further from it, so, the rejection fully comes from RSHEX+ and the number is 1.140 ± 0.006.

One comment about the HEX afterburner cut in the table. The rejection is 5% higher compared with the table-8, the difference is significant compared with the statistical fluctuation. The reason is that 1gamma trigger data sets (, precisely speaking $K_{\pi 2}(1)$ data with additional 1gamma trigger bits) are used when the measurement is done. They always have a photon hit in BV, thus, at least the photon pass through range stack counters, that makes HEX afterburner rejection higher.

Cut Names	# of events	rejection
all 1gamma trigger bits except for L1.2		
and all other setup cuts	5115	—
$\cdots$ + HEX after burner cut	4382	1.167 ± 0.007
$\cdots$ + L1.2 trigger bit	3845	1.140 ± 0.006

Table 27: RSHEX+ rejection is L1.2

Self veto by tagging photon splitting A tagging photon sometimes splits in its conversion process and makes a separate energy deposit, which is recognized as an another cluster and discarded by 2nd photon veto. This is a kind of self veto and must be corrected for an accurate measurement.

A MC based study was done for this. The following events are generated by MC; Kaon decays into $K^+ \to \pi^+\pi^0$ and the π^0 decays into $\pi^0 \to \gamma X$, where X is a massless, none interactive particle. In plain words, it is the same as $\pi \to \gamma\gamma$ occurs and one of the photons is removed ideally by cheating the MC source code. Because in those events, all kinematics are just $K_{\pi 2}$ and only one photon (and one pion) exists in the final state, if some events are discarded by the 2nd photon veto, they all are due to the photon splitting. To measure it more accurate, all analysis process is re-done with these events; the exact same setup cuts and the exact same photon reconstruction, $K_{\pi 2}$ event reconstruction codes are used.

Obviously, the self veto effect depends on its photon energy, the correction factor is described as $C_{\text{selfveto}}(\theta, E)$. The table-() is the result.

Overveto by accidtals test

4.12 Systematic errors in the table

4.12.1 Cell cross-talk matrix

4.12.2 Fake reconstruction

Accidentals

Muon backgrounds : $K_{\mu 2} + accidental, K_{\mu 2\gamma}$

4.13 Single photon detection inefficiency — Result —

The single photon detection inefficiency is obtained by extending the equation-11 to include correction factors.

$$\frac{N^{\text{numer}}(\theta, E)}{N^{\text{denom}}(\theta, E)} \times A_{\text{norm}} \times \frac{C_{\text{RSHEX+}}}{C_{\text{selfveto}}(\theta, E) C_{acc}} \tag{18}$$

The table - is the at acceptance = , the figure - is the plot showing them visually.

we can see the photo nuclear events surviving final cut in the band region

5 π^0 Detector Inefficiency in $K_{\pi 2}$ Decay

In this section, π^0 detection miss probability $P_{\pi^0\ \mathrm{miss}}$ will be convoluted from the single photon inefficiency table by following the equation-19.

$$P_{\pi^0\ \mathrm{miss}} = \sum_{i}^{N} \frac{P_{SPI}(\theta_1^i, E_1^i) P_{SPI}(\theta_2^i, E_2^i)}{N} \tag{19}$$

where $P_{SPI}(\theta, E)$ is the single photon inefficiency table, and θ_k^i, E_k^i is a direction and energy of the k-th photon in the i-th event, "k" is 1 or 2 because π^0 emits two photons and "i" is the event number which runs through 1 to N.

5.1 Daughter map generation

As seen in the single photon inefficiency tables, each cell has a center value $P_{SPI}(\theta, E)$ and its uncertainty $E_{SPI}(\theta, E)$. To properly estimate an uncertainty on π^0 detection inefficiency, the $E_{SPI}(\theta, E)$ must be correctly propagated to the π^0 inefficiency when the convolution is done. It is OK if the errors are also convoluted in the same way with a weight matrix from a MC phase space generator, but in this analysis, more robust and simple way of "daughter map method" is taken.

Daughter map Using a gaussian random number generator which follows N(μ, σ): $\mu = P_{SPI}(\theta, E)$, $\sigma = E_{SPI}(\theta, E)$, each cell content is replaced with a randomly generated number. That means the generated new map has a random fluctuation comparable amount of their error. This table is called a "daughter map". The most dominant error in the single photon inefficiency table is a statistical error (especially in high energy region) and in lower energy region, that is a resolution in the tagging photon measurement. The former follows a poisson statistics and the latter follows a gaussian distribution. But simply, only gaussian generator is used here.

In total, 500 different daughter maps are generated for each single photon inefficiency table, Since every daughter map gives us a different π^0 inefficiency, totally 500 different inefficiency estimations will be obtained from them. The most likely π^0 inefficiency is extracted from their mean value and its uncertainty is taken from their RMS.

5.2 MC phase space generation and trigger bias correction

Next, photon phase space (θ_k^i, E_k^i)s are required to be generated by MC. We are afraid a localization of the (θ_k^i, E_k^i) around particular SPI cells due to statistical shortage, about 6×10^6 events are generated by MC. And one more, in order to correctly reproduce real (θ_k^i, E_k^i) distribution, all trigger bias and the bias from setup cuts must be introduced properly. For example, since π^+ flight direction is restricted by a trigger acceptance in θ direction, that causes a bias in the photon (θ_k^i, E_k^i) through the constraint that π^0 always flights to a back-to-back direction of the π^+.

A blue histogram in the figure-() shows the π^+ dip angle distribution of real data made with "PNN w/o online PV" trigger. A cyan histogram is that of MC π^+ obtained with $K_{\pi 2}(1)$ trigger. The difference is extracted as a correction function and applied when the convolution is done.

5.3 Result

The figure- is a distribution of the convoluted π^0 inefficiency at the acceptance = xxx.

The figure- shows π^0 rejections from direct measurement in the section- and the estimated one in this section. They are well consistent with each other, and it can be said the π^0 inefficiency is well described by a photon detection inefficiency.

5.3.1 Rejection as a function of π^+ dip angle

As mentioned before, π^+ dip angle distribution is reflected in the photon (θ_k^i, E_k^i) distribution. This means, π^0 inefficiency has a functional dependence to the π^+ dip angle because the photon inefficiency P_{SPI} varies depending on the photon space space (θ, E). If the same dependence is observed in real data, this will be a strong evidence of the backgrounds comes from photon inefficiency and will be a proof of the obtained SPI table is correct.

The figure-() is the π^0 rejection as a function of π^+ dip angle. Both are consistent.

5.4 Discussion about the background mechanism

6 Background Expectation — 1/3 sample study

6.1 Expected number of backgrounds

6.2 Background distribution as a function of π^+ dip angle

6.3 Poisson based normal background subtraction

poisson distribution

6.4 Background subtraction with unbinned extended maximum likelihood

$$L = \frac{e^{-(s+b)}}{N!} \prod_{i}^{N} (sS_i + bB_i) \tag{20}$$

6.5 Chi square fitting

A fitting function $f(cos3d)$ is defined by a linear combination of the signal distribution $S(cos3d)$ and the background $B(cos3d)$.

$$f(cos3d) \equiv sS(cos3d) + bB(cos3d) \tag{21}$$

6.5.1 David's technique

Description	PNN1 PASS1 prescale 3		
Kin, TD, PV setup cuts Beam related setup cuts	UTCQUAL, RNGMOM, COS3D, LAYV14, ZFRF, ZUTOUT, PV (no TGPV) TGQUALT, TGZFOOL, TARGF, DTGTTP, RTDIF, DRP, KIC, BWTRS, B4ETCON, B4TRS, B4CCD, TIMCON, TGTCON, TIC entry : 2599150		
π^+, μ beam tag	B4ABM $<$ 1.0, PNN1BOX entry : 38290		
Misc. cuts	All Kin * All TD entry : 8283	All TD entry : 24546	— NO — entry : 38290
	DELC		
Rejection	entry : 0 —	entry : 1 24546 ± 24545	entry : 25 1531 ± 306

Table 28: Single beam background bifurcation study (Rejection branch) : 2/3 sample

7 Preparation for 2/3 smaple study

7.1 Number of backgrounds prediction for 2/3 samples

Description	PNN1 PASS1 prescale 3	
Kin, TD, PV setup cuts Beam related setup cuts	KP2BOX, UTCQUAL, RNGMOM, COS3D, LAYV14, ZFRF, ZUTOUT, PV (no TGPV) TGQUALT, TGZFOOL, TARGF, DTGTTP, RTDIF, DRP, KIC, B4DEDX, BWTRS, B4ETCON, B4TRS, B4CCD, B4EKZ, TIMCON, TGTCON, TIC entry : 10724	
Anti-Tag	$\overline{\text{DELC}}$ entry : 5793	
Make branches	[Kaon beam] CPITRS, CPITAIL entry : 845	[Pion beam] CKTRS, CKTAIL entry : 5097
All other cuts	B4DEDX, KIN, TD, PV, CKTRS, CKTAIL entry : 50	B4DEDX, KIN, TD, PV, CPITRS, CPITAIL entry : 50

Table 29: Single beam background bifurcation study (Normalization branch) : 2/3 sample

Description	PNN1 PASS1 prescale 3	
Kin, TD, PV setup cuts Beam related setup cuts	UTCQUAL, RNGMOM, COS3D, LAYV14, ZFRF, ZUTOUT, PV (no TGPV), TD TGQUALT, TGZFOOL, DELC, B4DEDX, B4ETCON, TIMCON entry : 244601	
Two beam tag	$\overline{\text{B4TRS,B4CCD}}$, PNN1BOX entry : 33014	
Make branches	[Kaon beam] CPITRS, CPITAIL entry : 771	[Pion beam] CKTRS, CKTAIL entry : 31047
Further cuts	$1.1 <$ B4ARS < 5.0 entry : 473	B4ARS $< 1.1, TGZ > -7.0$ entry : 18268
Rejection	BWTRS, CKTRS, CKTAIL entry : 11 43 ± 13	BWTRS, CPITRS, CPITAIL entry : 11 1661 ± 501

Table 30: Two beam background bifurcation study (Rejection branch) : 2/3 sample

Description	PNN1 PASS1 prescale 3	
Kin, TD, PV setup cuts	KP2BOX, UTCQUAL, RNGMOM, COS3D, LAYV14, ZFRF, ZUTOUT, PV (no TGPV)	
Beam related setup cuts	TGQUALT, TGZFOOL, TARGF, DTGTTP, RTDIF, DRP, DELC, KIC, B4DEDX, B4ETCON, B4EKZ, TIMCON, TGTCON, TIC entry : 16934	
Make branches	[Kaon beam] CPITRS, CPITAIL entry : 7298	[Pion beam] CKTRS, CKTAIL entry : 15614
Anti-Tag	$\overline{\text{BWTRS, CKTRS, CKTAIL}}$ entry : 974	$\overline{\text{BWTRS, CPITRS, CPITAIL}}$ entry : 9290
All other cuts	B4TRS, B4CCD, KIN, TD, PV	
	entry : 98	entry : 644

Table 31: Two beam background bifurcation study (Normalization branch) : 2/3 sample

Description	PNN1 PASS1 prescale 3	
Kin setup cuts	UTCQUAL, COS3D, LAYV14, ZFRF, ZUTOUT, PR_RF, PR_RF_XY, PR_RFZ1, PR_RFZ2, PV	
Beam related setup cuts	TGQUALT, TGZFOOL, TARGF, DTGTTP, RTDIF, DRP, DELC, KIC, B4DEDX, BWTRS, B4ETCON, B4TRS, B4CCD, CPITRS, CPITAIL, CKTRS, CKTAIL, B4EKZ, TIMCON, TGTCON, TIC entry : 101508	
Make branches	[Rejection branch]	[Normalization branch]
Further setup	$\overline{\text{RSDEDX}}$ Muon band : $231 < ptot < 250, rtot < 45$ Range tail : $190 < ptot < 231, rtot < 45$ $3. < rngmon\_new3 < 10.$ entry : 56675	PV, KP2BOX entry : 1099
Rejection — Inversion	TD entry : 75	$\overline{\text{TD}}$ entry : 377
	756 ± 87	KIN entry : 277

Table 32: $K_{\mu 2}$, μ background bifurcation study : 2/3 sample

Background type	Subcategory	# of events
Beam background	single beam	3.27×10^{-2}
	double beam (kaon entering)	2.28
	double beam (pion entering)	3.88×10^{-1}
Muon background	—-	3.66×10^{-1}
Total		3.066

Table 33: # of backgrounds in 2/3 sample

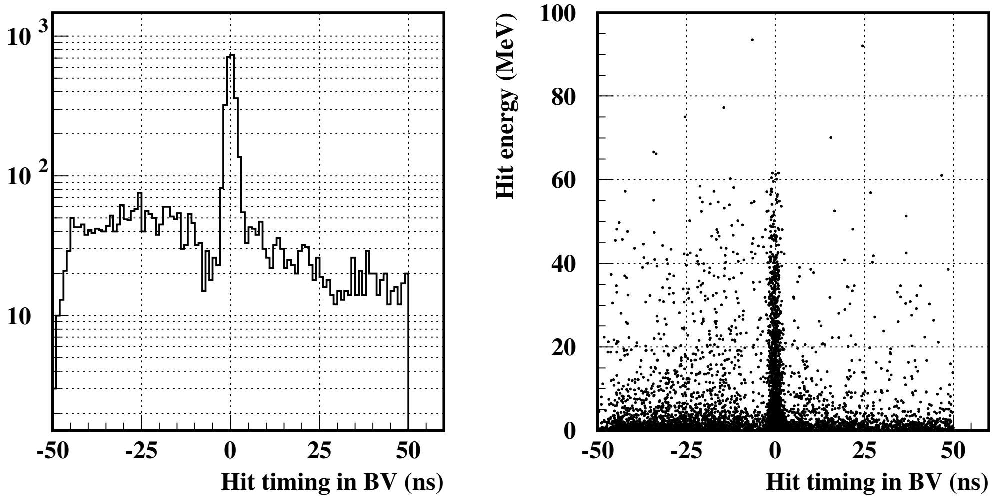

(a) BV early TDC hits

(b) BV early TDC hits vs their energy

Figure 1: BV early accidental hits

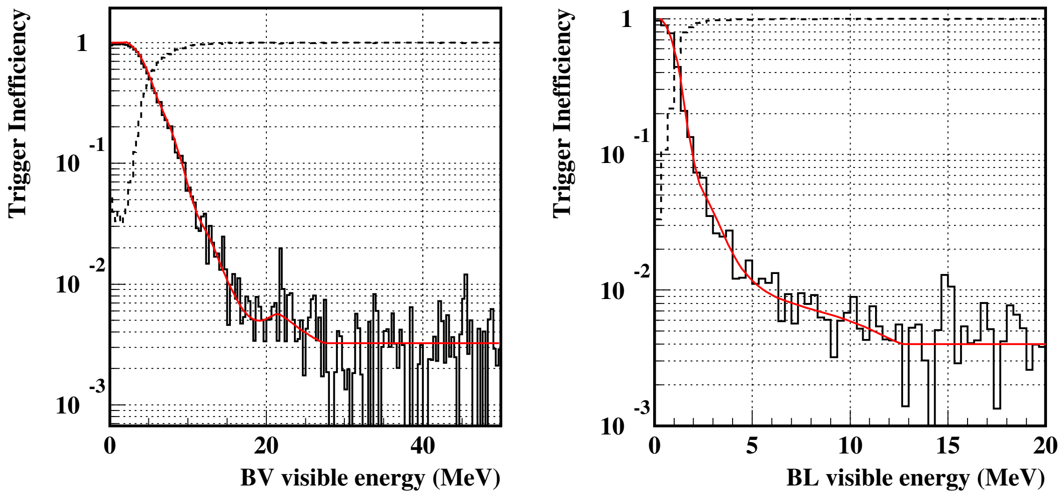

(a) Online BV trigger bit : ext(4)

(b) Online BVL trigger bit : ext(6)

dash line : trigger occupancy, solid line : trigger inefficiency, red line : a fitted curve to the inefficiency

Figure 2: Online BV,BVL trigger occupancy and inefficiency

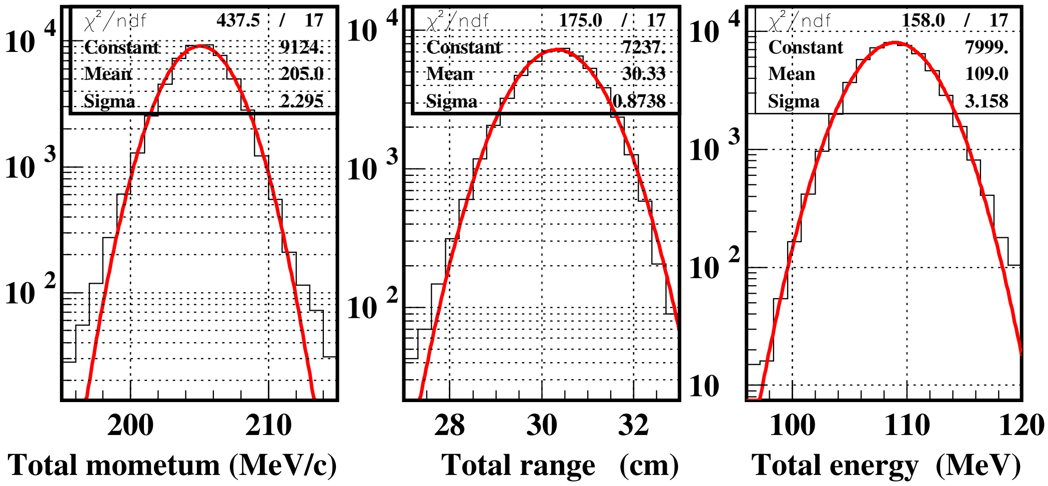

Figure 3: $K_{\pi 2}$-π^+ resolution. Total momentum, range, energy

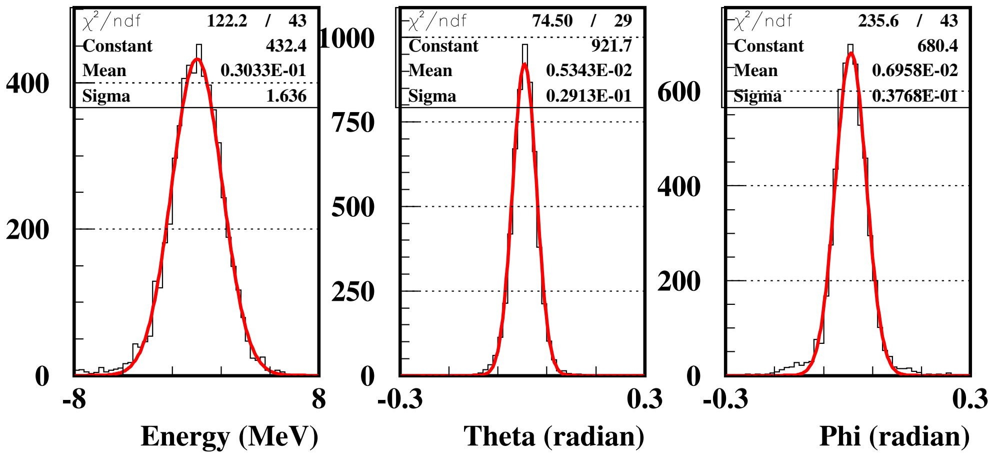

Figure 4: Tagging photon resolution (MC clustering raw). E_{tag}, θ, ϕ

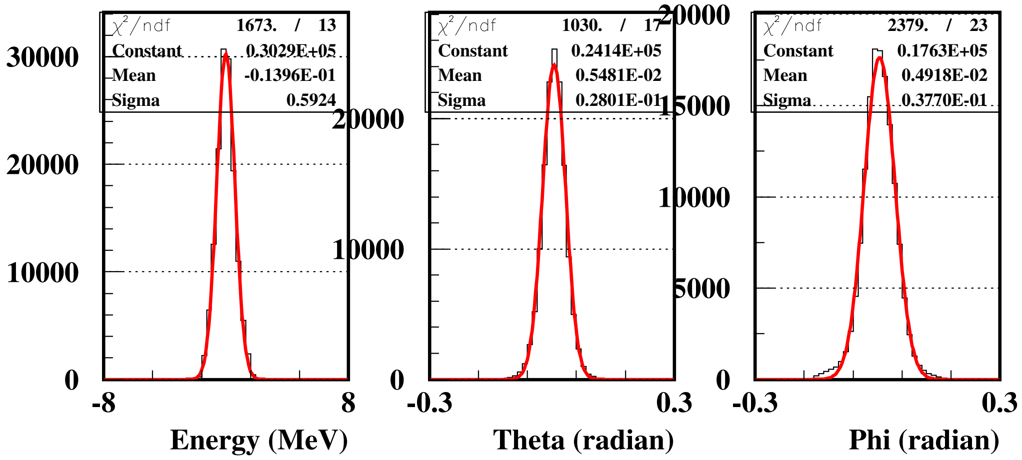

Figure 5: Tagging photon resolution (MC Lagrange multiplier fit). E_{tag}, θ, ϕ

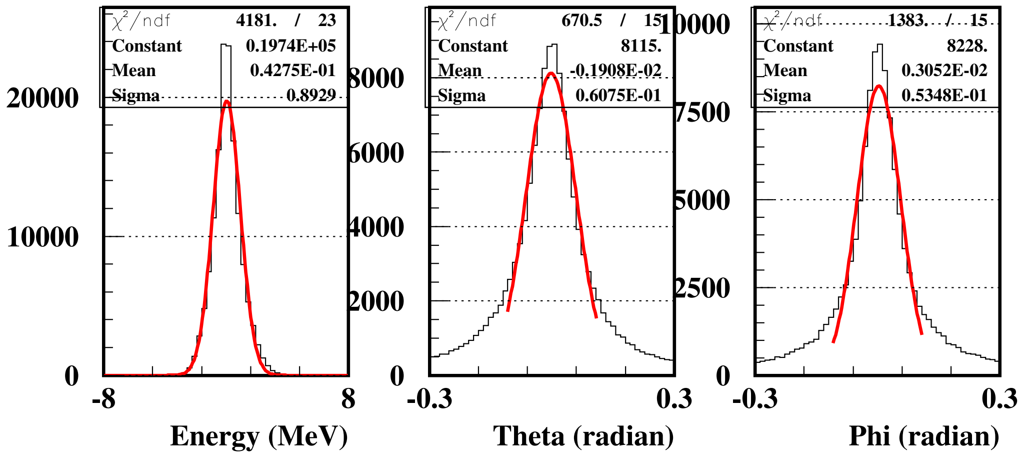

Figure 6: missing photon resolution (MC Lagrange multiplier fit). E_{tag}, θ, ϕ

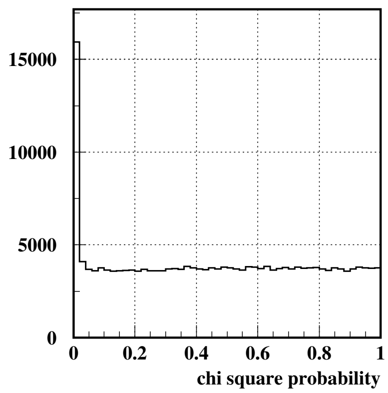

Figure 7: Chi square probability (MC recon)

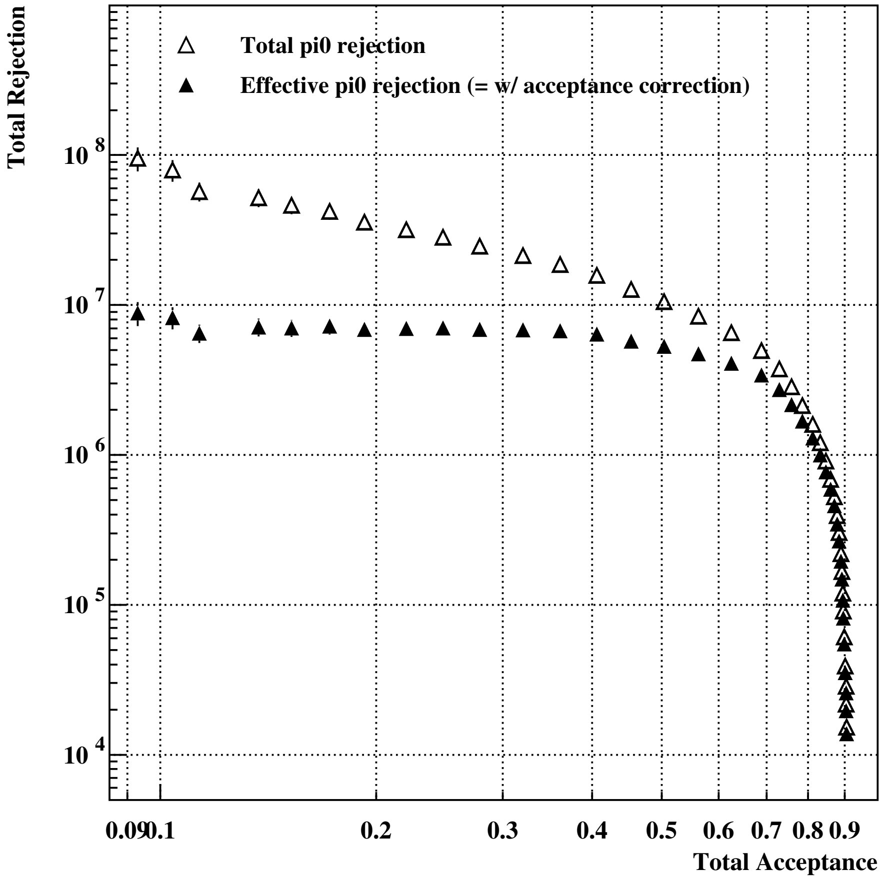

Figure 8: Total π^0 rejection vs acceptance profile curve